doi:10.1038/nature10143

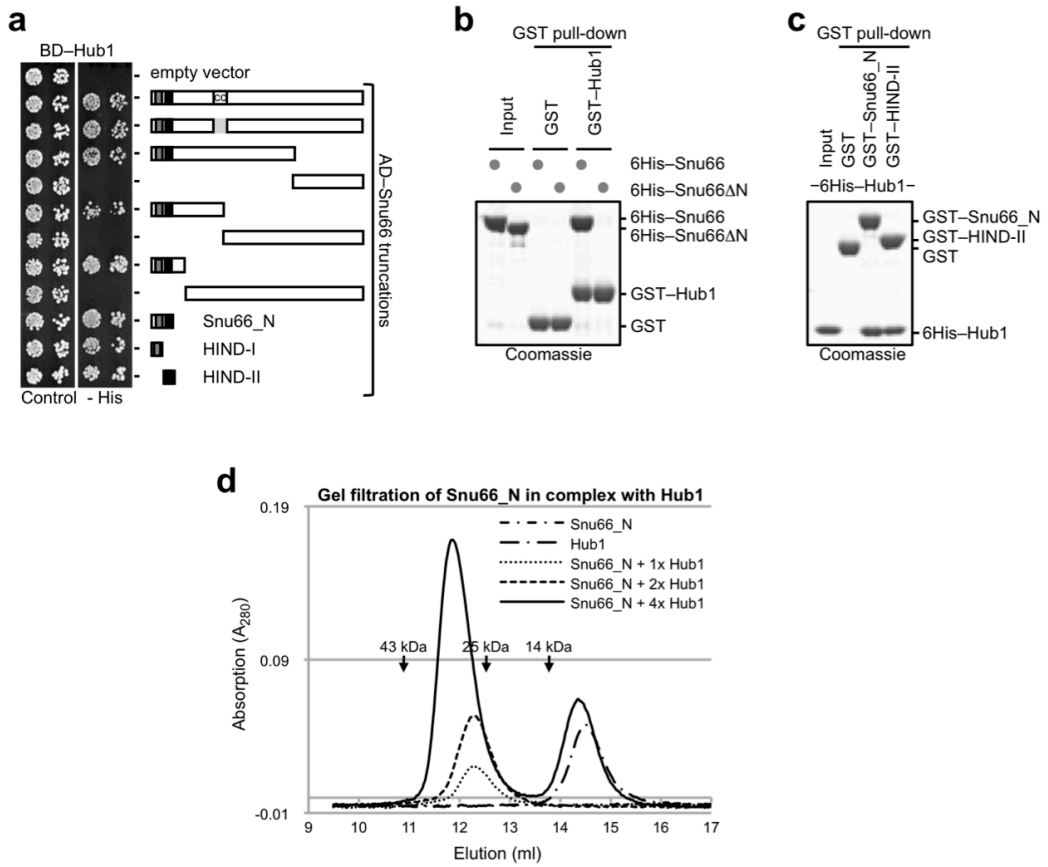

Supplementary Figure 1 | Hub1-Snu66 interactions in *S. cerevisiae*. a, Two-hybrid interaction between Hub1 and Snu66, and mapping of HINDs in Snu66. CC, putative coiled-coil region in Snu66 (BD, binding domain; AD activating domain of two-hybrid vectors). **b**, **c**, GST pull-down assays. Equimolar concentrations of indicated bacterially purified GST and 6His fusion proteins were mixed in PBS at 4°C. GST was used as control. Input represents one-third of the total proteins used in pull-down assays. Snu66ΔN lacks the N-terminal HIND sequences; Snu66_N is the N-terminal HIND-I and HIND-II harboring Snu66 fragment. **d**, Gel filtration of (HIND-I and HIND-II- bearing) Snu66 N-terminal domain (Snu66_N), Hub1, and mixtures of both, in 1:1 (Snu66_N:Hub1), 1:2, and 1:4 molar ratios. Size markers relative to elution volume are shown. Since Snu66_N lacks aromatic amino acids it does not absorb at 280nm, and hence its elution does not result in a peak at 280nm. For 1:1 and 1:2 molar ratios, only one peak for Snu66_N in complex with two Hub1 molecules (at ~30kDa) is observed. The two peaks for the 1:4 molar ratio represent the complex and free Hub1.

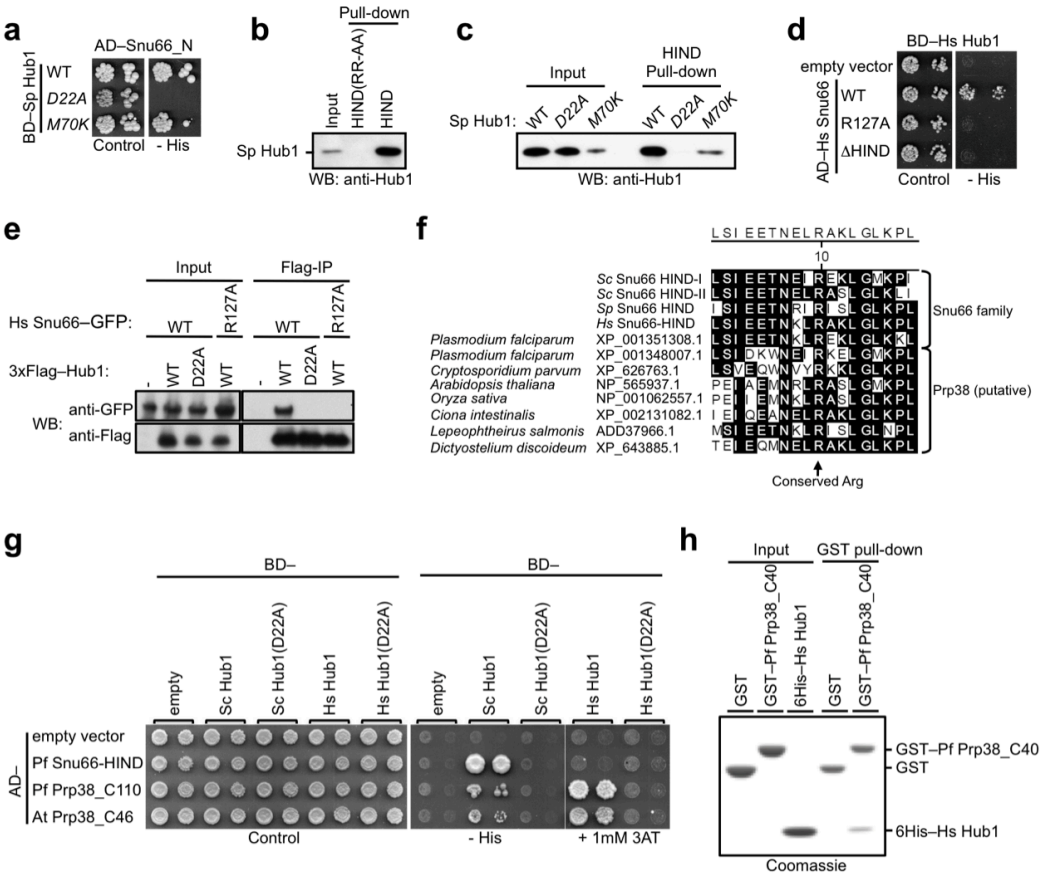

Supplementary Figure 2 | Hub1-HIND interactions in different eukaryotes. (*At, Arabidopsis thaliana; Hs, Homo sapiens; Pf, Plasmodium falciparum; Sc, Saccharomyces cerevisiae; Sp, Schizosaccharomyces pombe*). See Supplementary Figure 5 for the mutants of Hub1-HIND complex. **a**, Two-hybrid interaction between *Sp* Hub1 and *Sc* Snu66-HIND. Assays were performed with the indicated versions of *Sp* Hub1 fused to the Gal4-BD and *Sc* Snu66_N domain fused to the Gal4-AD. **b**, HIND pull-down of *Sp* Hub1. The N-terminal fragments of *Sc* Snu66 (with WT HIND sequences or its variant deficient in salt bridge-forming Arg residues HIND(RR-AA)) were covalently coupled to sepharose beads and used to pull-down *Sp* Hub1. Pull-down was performed from total cell lysate of *S. pombe* expressing *HUB1* driven by the *nmt1* promoter. **c**, Similar HIND pull-down, but of *Sp HUB1* WT, D22A and M70K variants (expression driven by the *nmt1* promoter). Note that Hub1(D22A) does not interact with HIND, whereas Hub1(M70K) (ref. [4]) does bind. **d**, Two-hybrid interaction between *Hs* Hub1 (UBL5) and *Hs* Snu66 (SART1). Constructs expressing WT *Hs SNU66* or its variants point-mutated or deleted of HIND (R127A or ΔHIND) were used. **e**, Immunoprecipitation (IP) of Flag-tagged *Hs* Hub1 from HEK 293T cells transiently transfected with *Hs HUB1*, WT or mutant variant D22A, in combination with GFP-tagged *Hs* Snu66, WT or HIND mutant variant R127A. Co-immunoprecipitation (co-IP) is monitored by anti-GFP and anti-Flag western blots. **f**, HINDs are present in proteins related to Snu66 and Prp38. ClustalW alignment of putative HINDs from different organisms. Multiple rounds of NCBI protein blast was performed using 18 aa long *Sc* Snu66-HIND peptides as query sequence (NCBI protein accession numbers refer to respective full length proteins). Arrow indicates the conserved Arg of HINDs essential for interaction with Hub1. **g**, Two-hybrid

interaction between *Sc* or *Hs* Hub1 and HIND containing fragments of *Pf* Snu66 (aa 8-25 of XP_001351308), *Pf* Prp38 (C-terminal 110 aa of XP_001348007.1) and *At* Prp38 (C-terminal 46 aa of NP_565937.1). Note that Hub1(D22A) does not interact with these HIND containing fragments indicating that the interaction mode is similar to Snu66-HINDs. **h,** GST pull-down assay to detect direct interaction between *Hs* Hub1 and *Pf* Prp38. Recombinant GST– fusion of *Pf* Prp38_C40 (C-terminal 40 aa of XP_001348007.1) was used to pull-down recombinant 6His-tagged *Hs* Hub1**.**

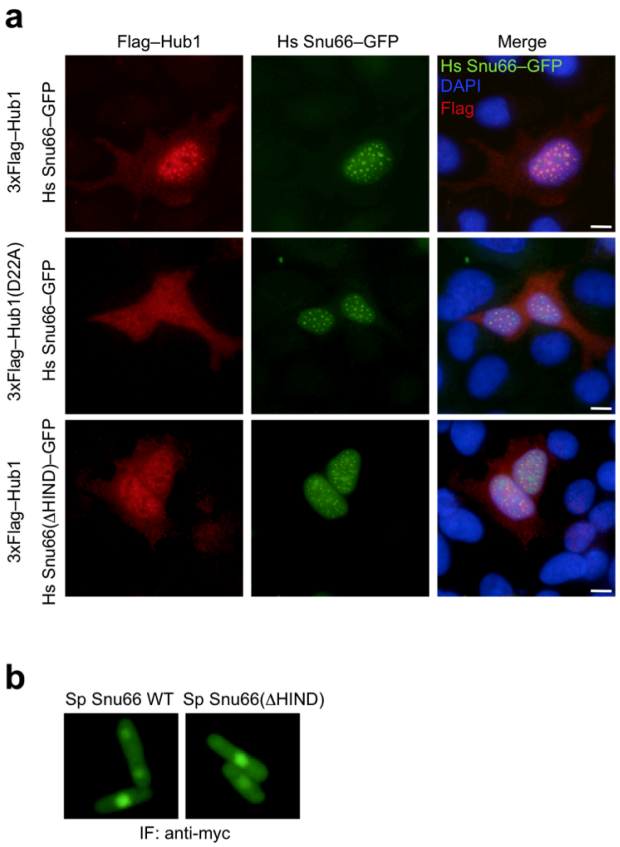

Supplementary Figure 3 | Localization of Hub1 and Snu66 in mammalian cells and *S. pombe*. a, Co-localization of *Hs* Hub1 and *Hs* Snu66 in nuclear speckles. Immunofluorescence of U2OS cells expressing *Hs* Snu66–GFP (green) and 3xFlag-tagged– *Hs* Hub1 (red). WT and mutant variants of *Hs* Hub1 and *Hs* Snu66 (Hub1(D22A), Snu66(ΔHIND)) were used. DAPI is used to stain DNA; the scale bar represents 10μm. WT Hub1 does not colocalize with Snu66 mutant (Snu66(ΔHIND)), and Hub1 mutant (Hub1(D22A)) does not colocalize with WT Snu66. **b**, Immunofluorescence of *S. pombe* strains expressing Myc-epitope tagged *Sp* Snu66 WT or mutant lacking HIND (ΔHIND) shows that Hub1-HIND interaction is not required for the nuclear localization[4] of Snu66.

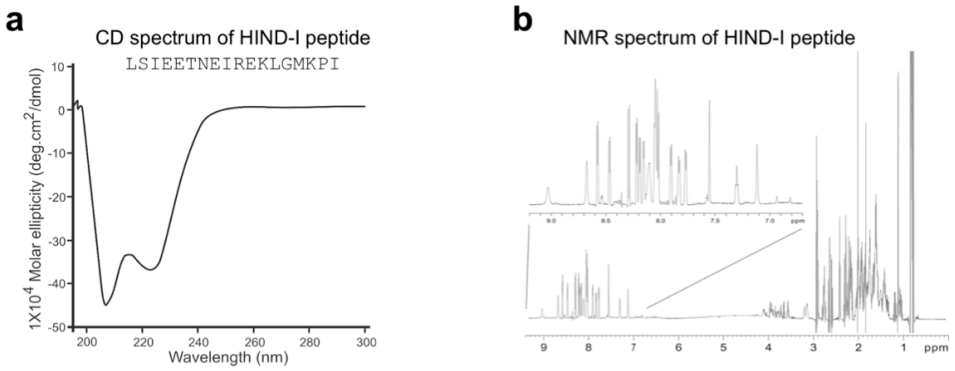

Supplementary Figure 4 | **Helical structure of free HIND-I in solution. a**, CD spectrum of HIND-I peptide. Molar CD spectrum of the 18 aa HIND-I peptide shows a spectrum typical for a helical protein with two characterestic minima for α-helix at about 209nm and 222nm. **b**, NMR spectrum of HIND-I peptide. 1D proton NMR spectrum of the HIND-I peptide showing dispersion in amide (~8.3ppm) region indicating that the peptide adopts a helical structure in solution.

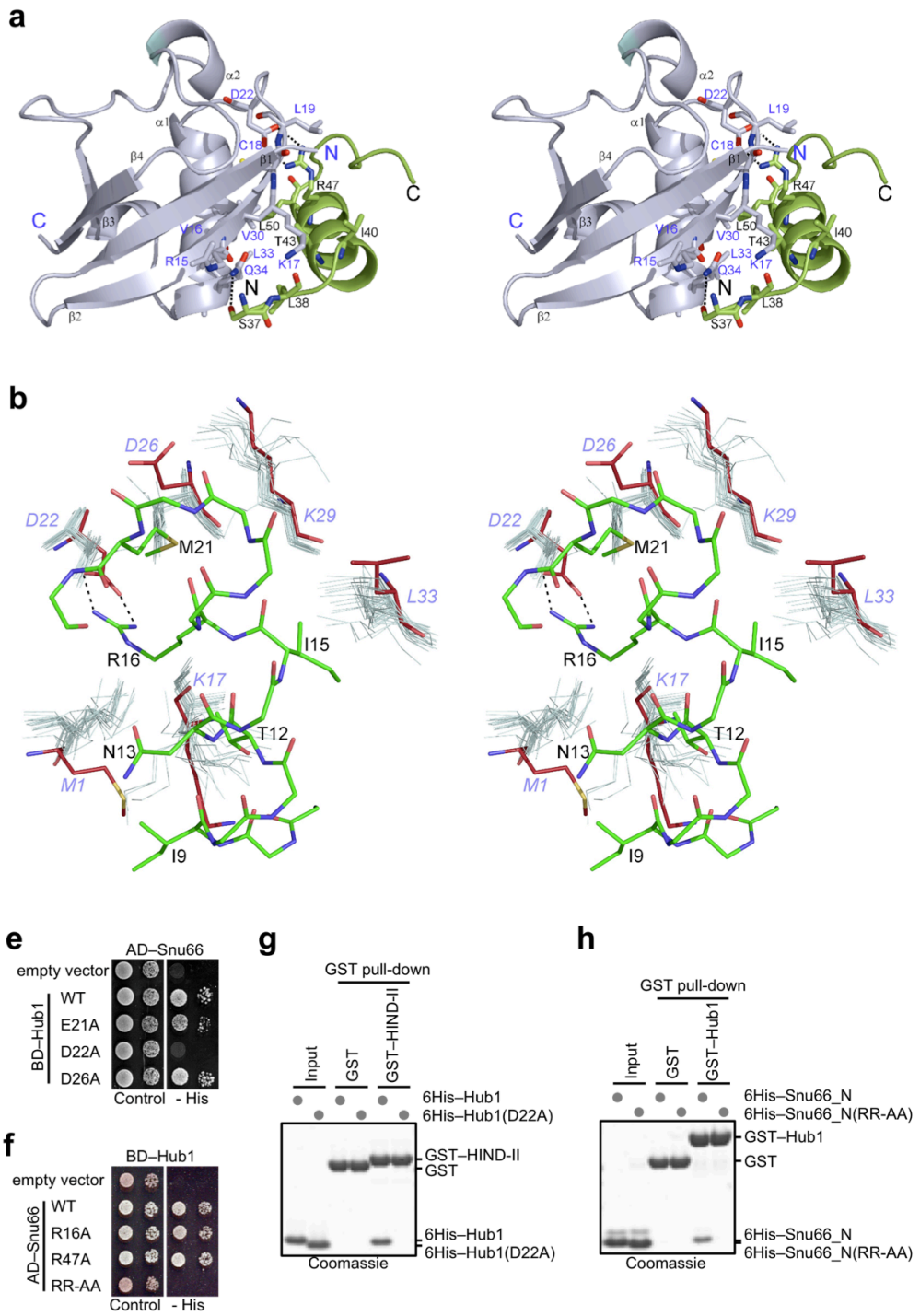

Supplementary Figure 5 | X-ray structures of HIND, Hub1, and Hub1-HIND complexes. a, Stereoplot of Hub1-HIND-II complex. The molecule is rotated by 180° along vertical axis from the orientation seen in Fig. 1e. Compared to HIND-I, HIND-II has two additional hydrogen bonds

between NH and Oγ of its Ser37 and the Hub1 Arg15 OH and Nε of Asn34, respectively. **b**, Upon HIND binding, Hub1 undergoes substantial induced-fit reorganization. Crystal structure of the complex (shown as sticks) is compared with NMR structure of free Hub1 (thin gray lines, PDB ID: 1M94). Met1 side chain of Hub1 is covering the binding interface of HIND-I, and is pointing towards Asp22. In both complexes with HIND-I or HIND-II this side chain is rotated away from binding site, thereby opening a pocket to accommodate HIND-I's Arg16 side chain bound to Asp22. Met21 of HIND-I mediates a hydrophobic interaction with Hub1; its binding causes Hub1 Asp26 to rotate its carboxyl group away from the interface. Similarly, Lys17 of Hub1 rotates away from the binding site to create a space for HIND-I's Thr12 Cγ. Leu33 of Hub1 is also rotated away from the binding interface to allow sufficient space for Ile15 of HIND-I. In complex, Hub1 Lys29 seems to be fixed at rotamer that points the side chain towards the solvent and far away from binding site. The structure of free Hub1 shows that this side chain is very flexible. **c-f,** Corroboration of Hub1-Snu66 interactions seen in the X-ray structures. **e, f,** Two-hybrid assay with WT and salt bridge defective variants of Hub1 and Snu66. Hub1 variants with other surface replacements were used as control (E21A, D26A). Snu66 and its variants that have Arg-Ala replacements in the two HINDs (R16A, R47A, and RR-AA = R16A R47A) were used as preys. (AD, activation domain; BD, DNA-binding domain of two-hybrid vectors). **g**, GST–HIND-II-mediated pull-down of recombinant Hub1 and Hub1(D22A), a salt bridge-defective variant (assay similar to Supplementary Fig. 1b, c). **h**, GST–Hub1-mediated pull-down of recombinant Snu66_N (HIND-I and HIND-II bearing N-terminal domain) or Snu66_N variant that have Arg-Ala replacements in the two HINDs of Snu66 (RR-AA = R16A R47A).

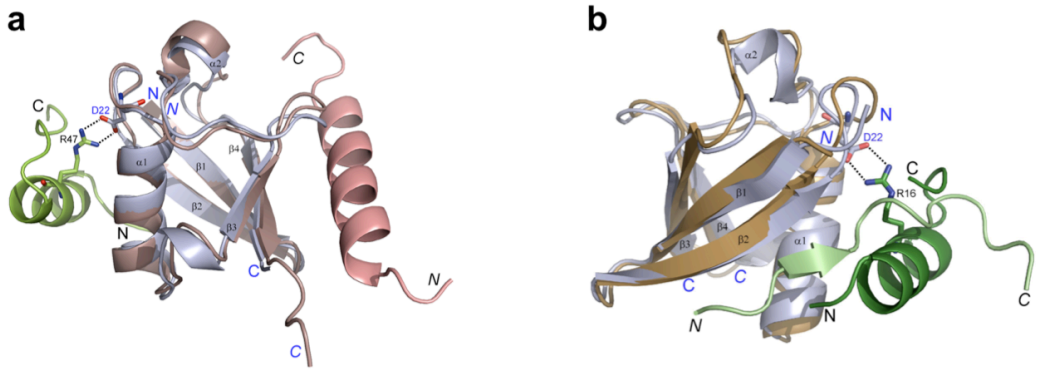

Supplementary Figure 6 | Comparison of Hub1-HIND complex with ubiquitin-UIM and SUMO-SIM complexes. a, Hub1-HIND-I interaction (blue, green) superimposed with ubiquitin-UIM (dark pink, pink) and **b**, SUMO-SIM (brown, green). The view in **(a)** is rotated 180° along vertical axis to that seen in **b**.

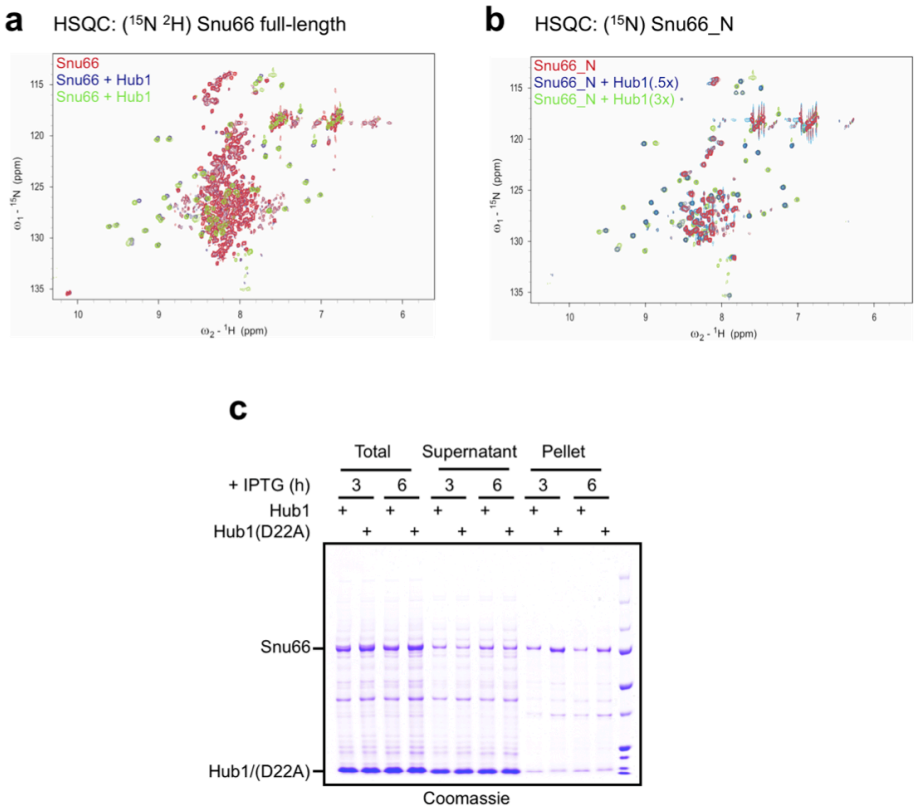

Supplementary Figure 7 | Hub1 binding induces partial folding of Snu66. a, **b**, HSQC spectrum of ^{15}N-labelled *Sc* Snu66_N and perdeuterated ^{15}N-labeled full-length *Sc* Snu66 (red spots) displays changes due to folding of several residues after addition of Hub1 (blue and green spots). Overlay of the spectra of the two complexes (Hub1-Snu66_N and Hub1-Snu66) shows that Hub1-induced folding is restricted to the N-terminal domain of Snu66. **c**, *Sc* Snu66 protein solubility assay in bacteria. *E. coli* BL21-RIL cells were co-transformed with pET28 vectors expressing 6xHis tagged *Sc* Snu66 and WT Hub1 or its mutant variant Hub1(D22A). Expression was induced by 1mM IPTG for the indicated time at 37°C. Following lysis of bacterial spheroplasts, soluble (supernatant) and insoluble (pellet) fractions from equal optical density of cells were analyzed by SDS-PAGE.

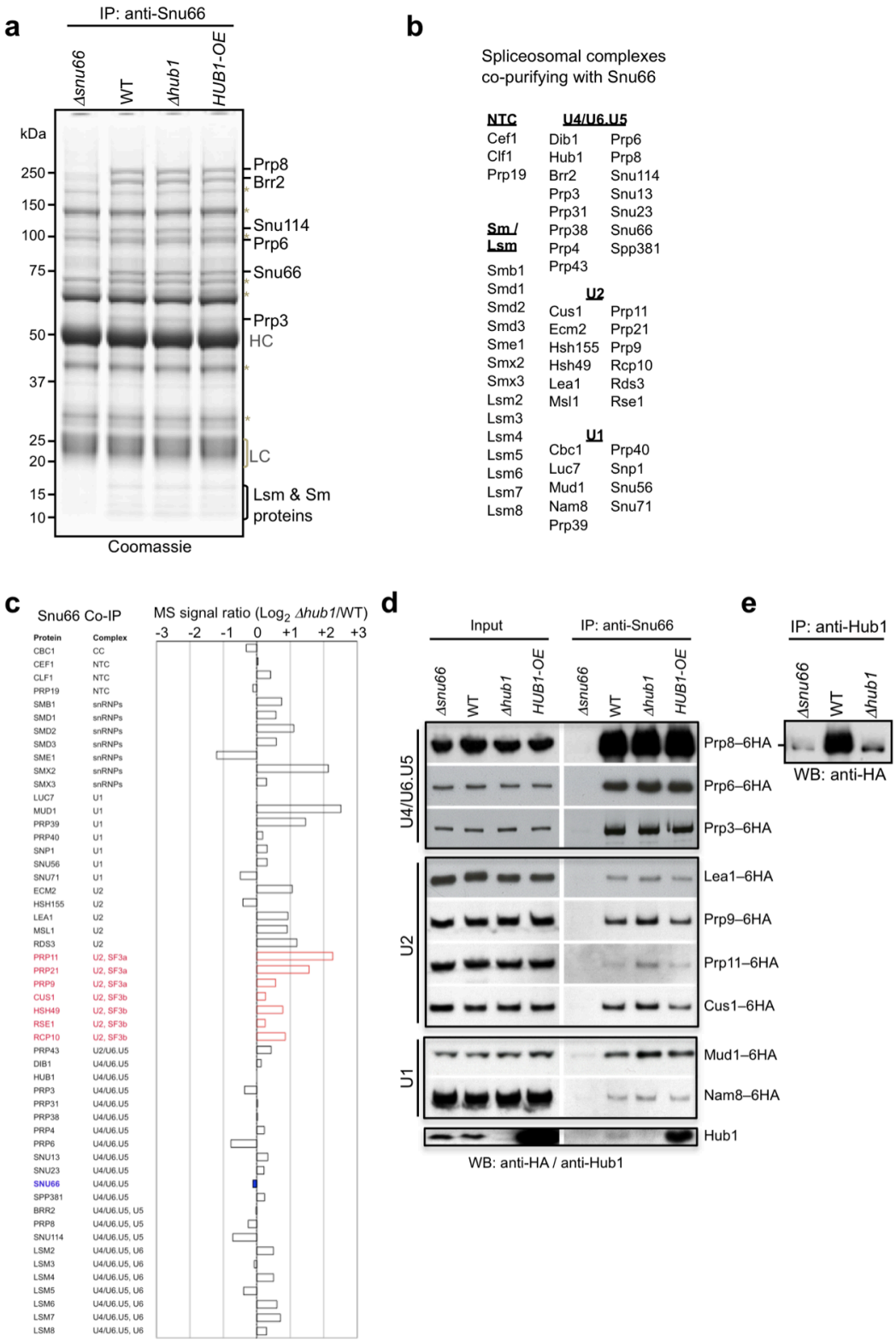
a
IP: anti-Snu66
Δsnu66
WT
Δhub1
HUB1-OE
kDa
250
150
100
75
50
37
25
20
15
10
Prp8
Brr2
Snu114
Prp6
Snu66
Prp3
HC
LC
Lsm & Sm proteins
Coomassie
b
Spliceosomal complexes co-purifying with Snu66
NTC
Cef1
Clf1
Prp19
Sm / Lsm
Smb1
Smd1
Smd2
Smd3
Sme1
Smx2
Smx3
Lsm2
Lsm3
Lsm4
Lsm5
Lsm6
Lsm7
Lsm8
U4/U6.U5
Dib1
Hub1
Brr2
Prp3
Prp31
Prp38
Prp4
Prp43
Prp6
Prp8
Snu114
Snu13
Snu23
Snu66
Spp381
U2
Cus1
Ecm2
Hsh155
Hsh49
Lea1
Msl1
Prp11
Prp21
Prp9
Rcp10
Rds3
Rse1
U1
Cbc1
Luc7
Mud1
Nam8
Prp39
Prp40
Snp1
Snu56
Snu71
c
Snu66 Co-IP
MS signal ratio (Log2 Δhub1/WT)
-3 -2 -1 0 +1 +2 +3
Protein
Complex
CBC1 CC
CEF1 NTC
CLF1 NTC
PRP19 NTC
SMB1 snRNPs
SMD1 snRNPs
SMD2 snRNPs
SMD3 snRNPs
SME1 snRNPs
SMX2 snRNPs
SMX3 snRNPs
LUC7 U1
MUD1 U1
PRP39 U1
PRP40 U1
SNP1 U1
SNU56 U1
SNU71 U1
ECM2 U2
HSH155 U2
LEA1 U2
MSL1 U2
RDS3 U2
PRP11 U2, SF3a
PRP21 U2, SF3a
PRP9 U2, SF3a
CUS1 U2, SF3b
HSH49 U2, SF3b
RSE1 U2, SF3b
RCP10 U2, SF3b
PRP43 U2/U6.U5
DIB1 U4/U6.U5
HUB1 U4/U6.U5
PRP3 U4/U6.U5
PRP31 U4/U6.U5
PRP38 U4/U6.U5
PRP4 U4/U6.U5
PRP6 U4/U6.U5
SNU13 U4/U6.U5
SNU23 U4/U6.U5
SNU66 U4/U6.U5
SPP381 U4/U6.U5
BRR2 U4/U6.U5, U5
PRP8 U4/U6.U5, U5
SNU114 U4/U6.U5, U5
LSM2 U4/U6.U5, U6
LSM3 U4/U6.U5, U6
LSM4 U4/U6.U5, U6
LSM5 U4/U6.U5, U6
LSM6 U4/U6.U5, U6
LSM7 U4/U6.U5, U6
LSM8 U4/U6.U5, U6
d
Input
IP: anti-Snu66
Δsnu66
WT
Δhub1
HUB1-OE
U4/U6.U5
U2
U1
Prp8–6HA
Prp6–6HA
Prp3–6HA
Lea1–6HA
Prp9–6HA
Prp11–6HA
Cus1–6HA
Mud1–6HA
Nam8–6HA
Hub1
WB: anti-HA / anti-Hub1
e
IP: anti-Hub1
Δsnu66
WT
Δhub1
WB: anti-HA

Supplementary Figure 8 | Hub1 modifies the spliceosome. a, Immunoprecipitation (IP) of Snu66 from *S. cerevisiae* WT cells, *Δhub1* mutants, and *HUB1* over-expressing (OE) cells. Co-immunoprecipitated proteins were run on an SDS-PAGE, each lane was cut in 9 pieces, and analyzed by Orbitrap mass spectroscopy (MS). Positions for light (LC) and heavy (HC) chain antibodies and spliceosomal proteins are indicated. Asterisks mark non-specific protein bands. Molecular weight markers are shown on the left. **b**, Catalogue of spliceosomal proteins co-purifying with *S. cerevisiae* Snu66. Groups represent spliceosomal sub-complexes. **c**, Log_2 ratio of total MS signal intensities of Snu66 associated proteins in *Δhub1* and WT yeast. Total intensity of MS signals obtained for indicated proteins in each lane was used to calculate the ratio. **d**, Selected proteins were tagged (at their genomic loci) at their C-termini with 6HA in *Δsnu66*, WT, *Δhub1* or *HUB1*-overexpressing (OE) strains. Snu66 IP was performed and co-IP of epitope-tagged proteins was analyzed by western blotting (WB) using anti-HA antibody. **e**, IP of endogenous Hub1 from Prp8–6HA tagged strains show Hub1-Prp8 interaction through Snu66.

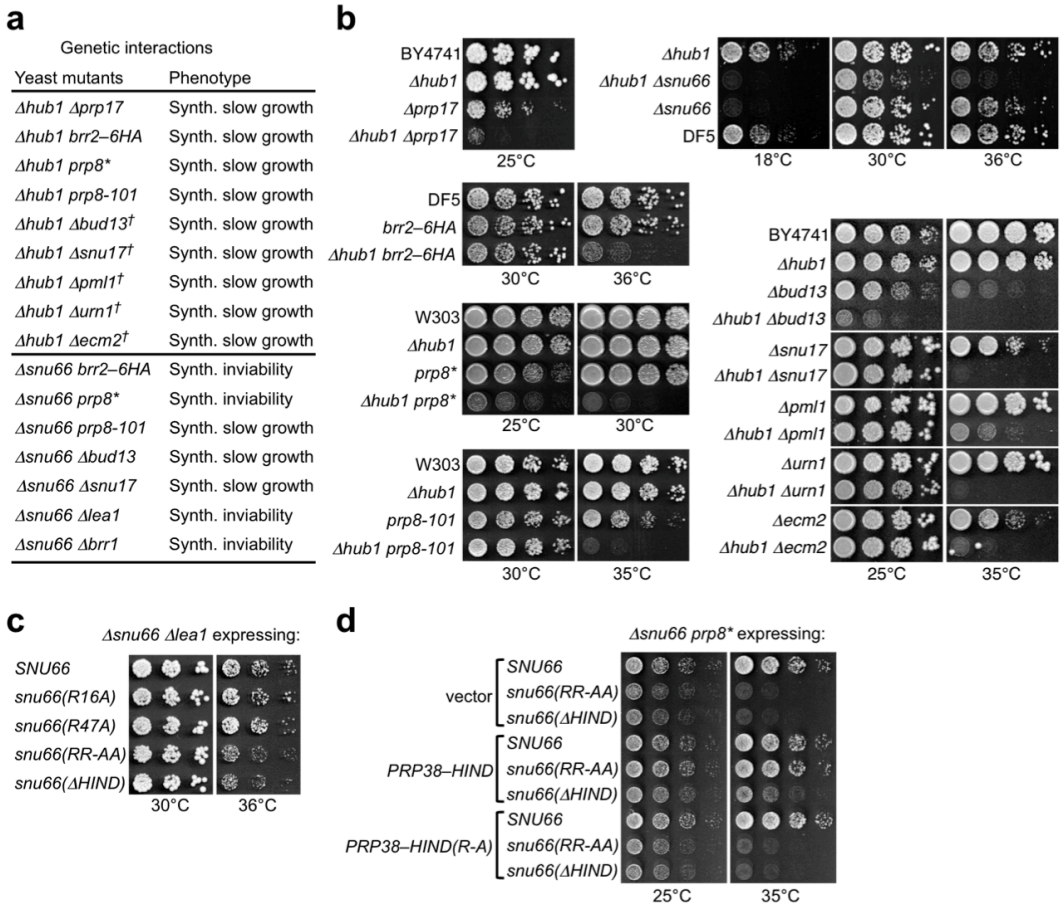

Supplementary Figure 9 | Genetic links to splicing in *S. cerevisiae*. a, b, Genetic interactors of *Δhub1* and *Δsnu66*. Synthetic growth phenotypes of double deletions relative to the corresponding single mutants are indicated. The cross symbol denotes confirmed genetic interactions of previously reported interactions identified by high-throughput studies[45,46]. The *prp8-101* allele was reported earlier[47]. The mutant *prp8** mutant (*prp8(P1384L)*) alone (allele provided by G. Dittmar; ref. [48]) is temperature sensitive, and the mutant *brr2–6HA* alone (the 6HA tag confers mutant phenotype) exhibits no obvious growth defect under the conditions tested. Mutant strains that did not show obvious synthetic growth defects with *Δhub1* are: *Δbrr1*, *Δcwc27*, *Δpml39*, *Δmlp1*, *Δmlp2, prp8-R1753K*, *prp8-161* and *prp8-162* (data not shown). Upper right panels in **(b)** show non-epistatic behavior of *Δhub1* and *Δsnu66* mutants from *S. cerevisiae*. **c**, Rescue of synthetic lethality of *Δsnu66 Δlea1* by expression of WT *SNU66* or mutant alleles. The synthetic lethality of *Δsnu66 Δlea1* could not be fully complemented by expression of *snu66* variants defective in Hub1 binding. **d**, Rescue of synthetic sickness (Fig. 2b) of *prp8* snu66* (*snu66(ΔHIND)*, *snu66(RR-AA)*) double mutants by a *PRP38–HIND* fusion (a DNA sequence encoding the HIND peptide LSIEETNKLRAKLGLKPL was fused upstream of the stop codon of *Sc PRP38*) but not by a *PRP38–HIND(R-A)* mutant deficient in Hub1 binding.

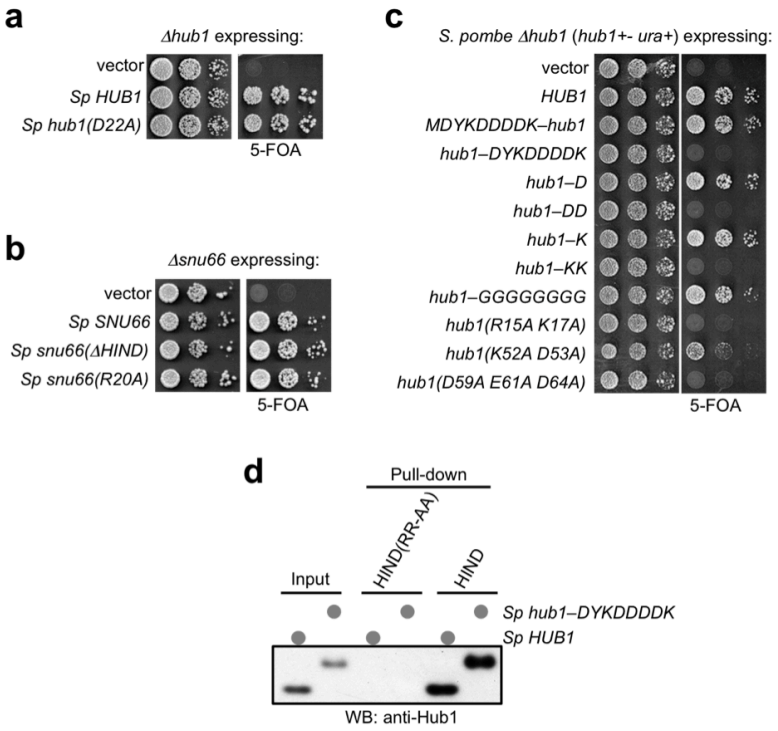

Supplementary Figure 10 | Complementation of *S. pombe Δhub1* and *Δsnu66*. a, Lethality of *S. pombe Δhub1* strain and complementation by *Sp HUB1* (WT) but also *hub1(D22A)*, indicating that Hub1-Snu66 interaction is not essential for viability in *S. pombe*. WT *HUB1* (expressed from a *URA4*-bearing plasmid[8]) was shuffled out by counter-selection on 5-FOA plates. For complementation assays, WT and mutant *HUB1* was expressed from the weak *nmt81* promoter. **b**, Lethality of *S. pombe Δsnu66* strain is complemented by *Sp snu66(ΔHIND)* and *snu66(R20A)*, indicating Snu66-Hub1 interaction is not essential for viability in *S. pombe*. Assay was performed as in **(a)**. **c**, Complementation assay using *S. pombe Δhub1* (lethal) by expression of Hub1 variants. *hub1(R15A K17A)*, *hub1(K52A D53A)*, *hub1(D59A E61A D64A)* are variants of Hub1 itself; all others are either N- or C-terminal extensions. Note that N-terminal extensions, or C-terminal extensions by a poly-Gly track or single charged residues (*hub1–D*, *hub1–K*) give rise to functional Hub1, as indicated by this complementation assay. By contrast, additions by two charged residues (*hub1–DD*, *hub1–KK*) lead to non-functional Hub1. **d**, Pull-down of *Sp* Hub1 with HIND (*Sc* Snu66_N) beads from total cell lysates of *S. pombe* strains expressing Hub1 or its variant with a C-terminal extension. Hub1 variant with the C-terminal extension was not defective in HIND binding. HIND(RR-AA) was used as negative control.

a RT-qPCR: Unspliced/Total RNA

Transcript	WT	*Δhub1*
ACT1	0.003	0.005
BET1	0.260	0.263
RPL7A-Int2	0.016	0.019
RPL30	0.040	0.096
RPL34B	0.015	0.094
UBC9	0.137	0.143

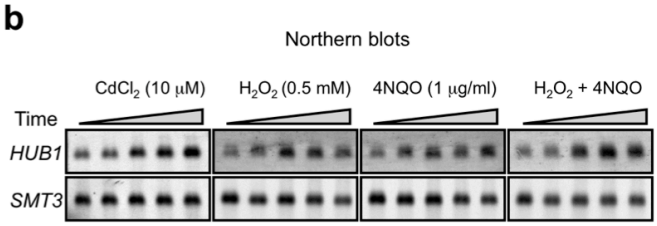

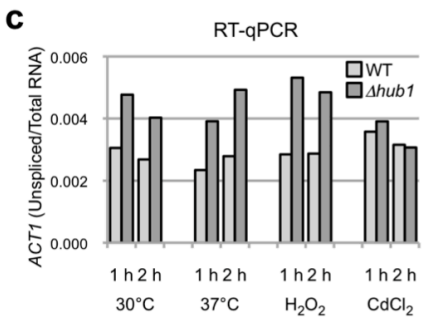

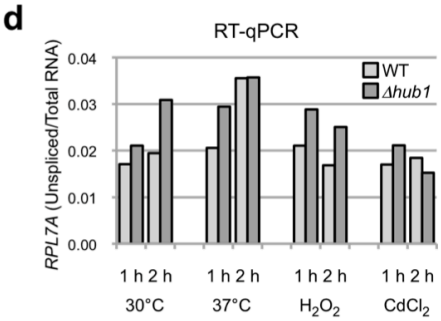

Supplementary Figure 11 | Role of Hub1 in general splicing. a, Confirmation of microarray results shown in Fig. 2c by quantitative RT-PCR. Splicing of selected transcripts presented as the ratio of unspliced (intron-containing) RNA to total RNA. RT reaction was performed using random hexamer primer and qPCR for unspliced and total RNA, respectively, was performed using forward primers annealing in intron and exon-2 with a common reverse primer annealing in exon-2. Average of three qPCR runs for intron-containing transcripts were divided with the average calculated for total cognate RNA. Note that the ratios of unspliced transcripts to total RNA are very low (the ratio of unspliced transcripts to total RNA is less than 1), but higher than WT levels of unspliced transcripts of *RPL30* (which is regulated by a feed-back loop[49]) and *RPL34B* are detected in *Δhub1* strain. **b**, *HUB1* transcripts are inducible under certain stress conditions. Northern blot of *Sc HUB1* mRNA levels after treatment with $CdCl_2$, H_2O_2, 4-nitroquinoline 1-oxide (4NQO; generates DNA double strand breaks), and H_2O_2 combined with 4NQO. *SMT3* (SUMO) was probed for control. Treatment was done for 15, 30, 60, and 120min (15μg of total RNA). **c, d,** General splicing defects in *Δhub1* yeast is not significantly aggravated upon stress treatment. Splicing of *Sc ACT1* and *RPL7A* transcripts under different stress conditions. Total RNA was isolated from yeast treated with H_2O_2, $CdCl_2$, and 37°C for 1 or 2h. Assay similar to **(a)**. The ratios of unspliced transcripts to total RNA remain very low.

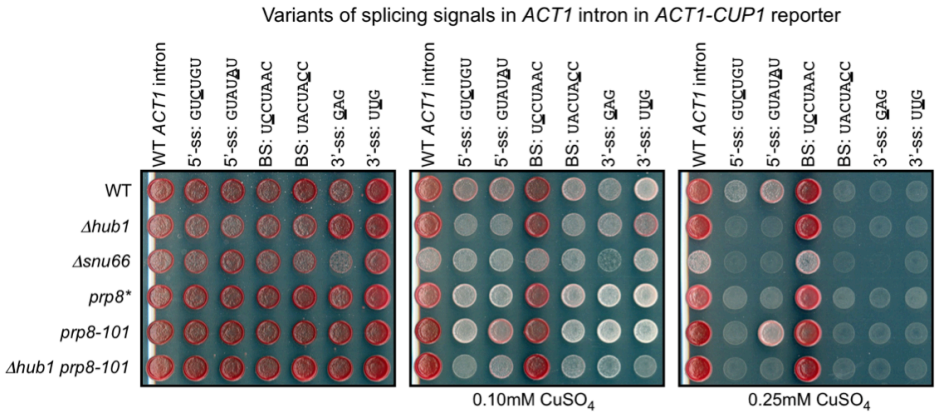

Supplementary Figure 12 | Defects in splice site (ss) usage. Splicing assay with an intron-containing *ACT1-CUP1* reporter[24]. Yeast strains (see Supplementary Figure 9) were transformed with *ACT1-CUP1* constructs harboring different 5'-, 3'-ss or branch point (BS) mutations. Changes of the splicing signals in *S. cerevisiae ACT1* intron are underlined (*ACT1* intron has 5'-ss: GUAUGU, 3'-ss: UAG, and BS: UACUAAC). Equal optical density of cells was spotted on plates containing various concentrations of $CuSO_4$ to monitor *CUP1* (copper metallothionein) activity. Plates were incubated at 30°C for 3 days.

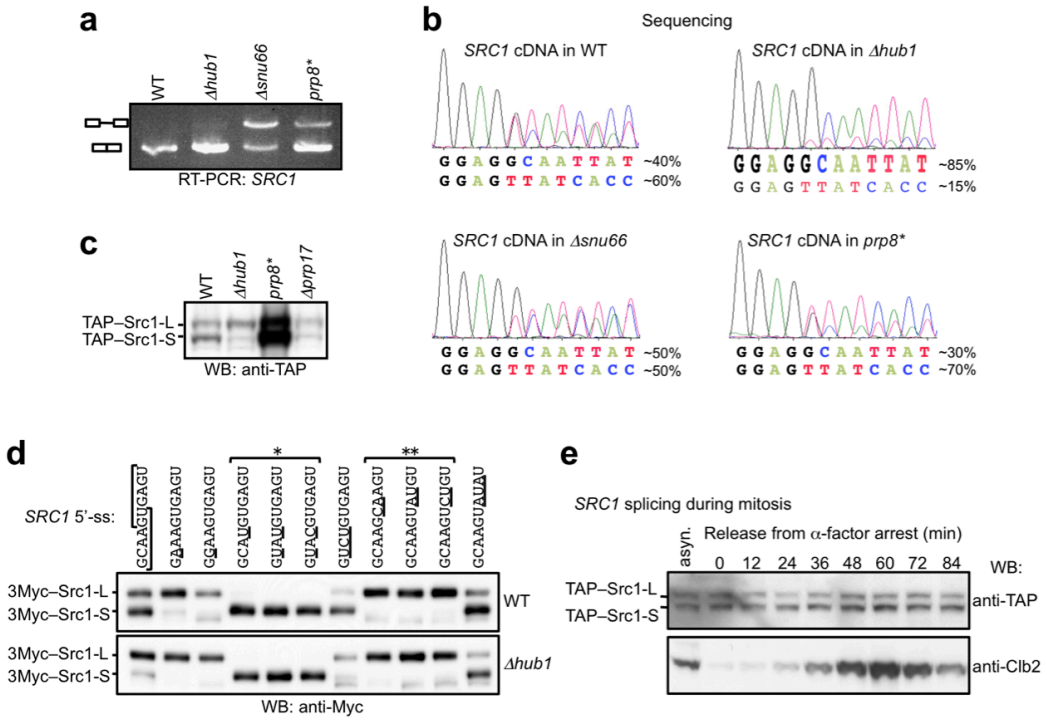

Supplementary Figure 13 | Defects in 5'-ss usage and alternative *SRC1* splicing. a, b, RT-PCR assay of *SRC1* transcripts **(a)**, and sequencing **(b)** of *SRC1* cDNA across exon1-intron boundaries in WT, *Δhub1*, *Δsnu66* and *prp8** (ref. [48]) mutants. Alternative *SRC1* splicing is most strongly affected in *Δhub1* strain, whereas other mutants possess both cDNAs (percentage abundance is estimated by integrating amplitudes of the sequencing peaks). Part of this figure is also shown in Fig. 4a. **c,** Alternative splicing of *SRC1* in indicated yeast mutants detected by western blot analysis of TAP–Src1. **d,** Alternative splicing of 5'-ss variants of *SRC1* in WT and *Δhub1* strain. A *CEN* plasmid was used to express 5'-ss variants of N-terminally 3Myc-tagged full-length *SRC1* via the *GAL1-10* promoter. *GAL* promoter was induced for 30min using 2% galactose. The changes introduced into the 5'-ss of *SRC1* are underlined; brackets denote mutations of the 5'-ss that lead to Hub1-independent splicing via the upstream 5'-ss (single asterisk) or the downstream 5'-ss (double asterisk). **e,** Usage of 5'-ss of *SRC1* pre-mRNA may be altered during cell cycle. Following 2h α-factor arrest of TAP–Src1 yeast, aliquots of culture at indicated time points were processed for western blot analysis. Cyclin level (WB: anti-Clb2) was used to monitor cell cycle progression.

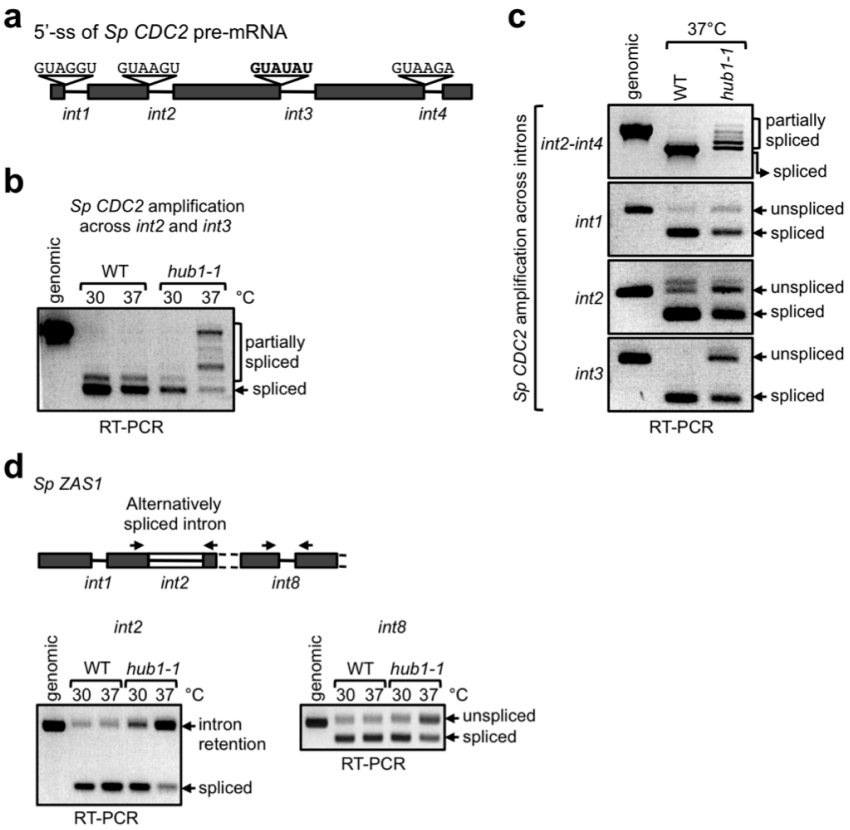

Supplementary Figure 14 | Defects in 5'-ss usage and alternative splicing in *S. pombe hub1* mutant. a-c, Splicing of introns in *Sp CDC2* pre-mRNA. **a,** 5'-ss of *CDC2* introns. **b,** RT-PCR assays of splicing across *int2* and *int3* in *CDC2* pre-mRNA show intermediate size products in *Sp hub1-1* strain[8] (37°C treatment for 3h), which likely results from intron retention or partial splicing, as monitored by PCR products across individual introns (detection by agarose gel electrophoresis) **(c)**. Note that splicing of *int3* with the 5'-ss GUAUAU is particularly affected in *hub1-1* allele. **d,** RT-PCR assay for products resulting from retention of an alternative intron (*int2*) in *Sp ZAS1*[30]. In the *hub1-1* mutant, splicing of *int8* harboring the *S. pombe* canonical 5'-ss GUAAGU was affected to a lesser degree than *int2* (the estimated ratio of 37°C PCR signal for *hub1-1* to WT was 2.7 fold for *int8* and 5.5 fold for *int2*).

Supplementary Table 1 | *S. cerevisiae* and *S. pombe* strains used in this study

Strain	Relevant Genotype	Reference
	Saccharomyces cerevisiae strains	
BY4741	*ura3Δ0 leu2Δ0 his3Δ1 met15Δ0*	50
BY4741	BY4741 deletion strains: *bud13::KanMX6; snu17::KanMX6; pml1::KanMX6; urn1::KanMX6; ecm2::KanMX6*	50
BY5563	*can1Δ::MFA1pr-HIS3 lyp1Δ ura3Δ0 leu2Δ0 his3Δ1 met15Δ0*	50
DF5/Y0003	*MAT***a** *trp1-1 ura3-52 his3Δ200 leu2-3,11 lys2-801 CAN1 BAR1*	51
PJ69-7A	*trp1-901 leu2-3,112 ura3-53 his3-200 gal4 gal80 GAL1::HIS3 GAL2-ADE2 met2::GAL7-lacZ*	52
W303/Y0226	*ho ade2-1 his3-11, 15 leu2-3, 112 ura3 trp1-1 ssd1 can1-100*	K. Nasmyth
Y0679	*DF5α hub1::LEU2*	7
Y0680	*DF5a hub1::LEU2*	7
YJU75	*MATa ade2 cup1Δ::ura3 his3 leu2 lys2 prp8Δ::LYS2 trp1:pJU169*	47
YM21	*DF5a hub1::LEU2 snu66::KanMX6*	This study
YM45	*DF5a/α lea1::natNT2 snu66::KanMX6*	This study
YM46	*DF5a/α brr1::natNT2 snu66::KanMX6*	This study
YM48	*DF5a/α snu17::natNT2 snu66::KanMX6*	This study
YM50	*DF5a/α npl3::natNT2 snu66::KanMX6*	This study
YM54	*BY5563 snu66::kanMX6*	This study
YM68	*DF5a snu66::KanMX6*	This study
YM69	*DF5α snu66::KanMX6*	This study
YSKM171	*DF5α BRR2–6HA::natNT2*	This study
YSKM174	*DF5α hub1::klTRP1*	This study
YSKM175	*DF5α YI211pTEF2-HUB1-tADH*	This study
YSKM179	*DF5α snu66::klTRP1 PRP3–6HA::natNT2*	This study
YSKM180	*DF5α PRP3–6HA::natNT2*	This study
YSKM181	*DF5α hub1::klTRP1 PRP3–6HA::natNT2*	This study
YSKM183	*DF5α snu66::klTRP1 PRP6–6HA::natNT2*	This study
YSKM184	*DF5α PRP6–6HA::natNT2*	This study
YSKM185	*DF5α hub1::klTRP1 PRP6–6HA::natNT2*	This study
YSKM186	*DF5α YI211pTEF2-HUB1-tADH PRP6–6HA::natNT2*	This study
YSKM187	*DF5α snu66::klTRP1 LEA1–6HA::natNT2*	This study
YSKM188	*DF5α LEA1–6HA::natNT2*	This study
YSKM189	*DF5α hub1::klTRP1 LEA1–6HA::natNT2*	This study
YSKM190	*DF5α YI211pTEF2-HUB1-tADH LEA1–6HA::natNT2*	This study
YSKM191	*DF5α snu66::klTRP1*	This study
YSKM193	*DF5α YI211pTEF2-HUB1-tADH PRP3–6HA::natNT2*	This study
YSKM195	*DF5a/α snu66::KanMX6 BRR2–6HA::natNT2*	This study
YSKM199	*DF5α hub1::klTRP1 BRR2–6HA::natNT2*	This study

YSKM250	*W303a hub1::KanMX6*	This study
YSKM252	*W303a snu66::KanMX6*	This study
YSKM283	*DF5α PRP8–6HA::natNT2*	This study
YSKM284	*DF5α hub1::klTRP1 PRP8–6HA::natNT2*	This study
YSKM285	*DF5α snu66::klTRP1 PRP8–6HA::natNT2*	This study
YSKM286	*DF5α YI211pTEF2-HUB1-tADH PRP8–6HA::natNT2*	This study
YSKM287	*W303α snu66::KanMX6*	This study
YSKM288	*W303a prp8**	G. Dittmar
YSKM294	*W303α prp17:natNT2*	This study
YSKM295	*W303a/α snu66::KanMX6 prp8**	This study
YSKM303	*W303a hub1::KanMX6 prp17::natNT2*	This study
YSKM307	*DF5α MUD1–6HA::natNT2*	This study
YSKM308	*DF5α hub1::klTRP1 MUD1–6HA::natNT2*	This study
YSKM309	*DF5α YI211pTEF2-HUB1-tADH MUD1–6HA::natNT2*	This study
YSKM310	*DF5α snu66::klTRP1 MUD1–6HA::natNT2*	This study
YSKM312	*DF5α PRP9–6HA::natNT2*	This study
YSKM313	*DF5α hub1::klTRP1 PRP9–6HA::natNT2*	This study
YSKM314	*DF5α YI211pTEF2-HUB1-tADH PRP9–6HA::natNT2*	This study
YSKM315	*DF5α snu66::klTRP1 PRP9–6HA::natNT2*	This study
YSKM321	*W303α prp8**	This study
YSKM324	*DF5α PRP11–6HA::natNT2*	This study
YSKM325	*DF5α hub1::klTRP1 PRP11–6HA::natNT2*	This study
YSKM326	*DF5α YI211pTEF2-HUB1-tADH PRP11–6HA::natNT2*	This study
YSKM327	*DF5α snu66::klTRP1 PRP11–6HA::natNT2*	This study
YSKM332	*DF5α NAM8–6HA::natNT2*	This study
YSKM333	*DF5α hub1::klTRP1 NAM8–6HA::natNT2*	This study
YSKM334	*DF5α YI211pTEF2-HUB1-tADH NAM8–6HA::natNT2*	This study
YSKM335	*DF5α snu66::klTRP1 NAM8–6HA::natNT2*	This study
YSKM340	*DF5α CUS1–6HA::natNT2*	This study
YSKM341	*DF5α hub1::klTRP1 CUS1–6HA::natNT2*	This study
YSKM342	*DF5α YI211pTEF2-HUB1-tADH CUS1–6HA::natNT2*	This study
YSKM343	*DF5α snu66::klTRP1 CUS1–6HA::natNT2*	This study
YSKM368	*W303a hub1::KanMX6 prp8**	This study
YSKM369	*W303α hub1::KanMX6 prp8**	This study
YSKM421	*YJU75 hub1::natNT2*	This study
YSKM422	*YJU75 snu66::natNT2*	This study
YSKM434	*YJU75 prp8-101*	47
YSKM435	*YJU75 prp8-101 hub1::natNT2*	This study
YSKM443	*W303a* P_{CUP1-1}*TAP–SRC1::natNT2*	This study
YSKM444	*W303a hub1::KanMX6* P_{CUP1-1}*TAP–SRC1::natNT2*	This study
YSKM445	*W303a snu66::KanMX6* P_{CUP1-1}*TAP–SRC1::natNT2*	This study

YSKM447	*W303a prp8* P_{CUP1-1}TAP–SRC1::natNT2*	This study
YSKM449	*W303a P_{CUP1-1}TAP–SRC1::KanMX6*	This study
YSKM451	*W303a P_{CUP1-1}TAP–SRC1::KanMX6 PRP38–HUB1::natNT2*	This study
YSKM452	*W303a P_{CUP1-1}TAP–SRC1::KanMX6 PRP38–hub1(D22A)::natNT2*	This study
YSKM453	*W303a P_{CUP1-1}TAP–SRC1::KanMX6 PRP38–hub1–DD::natNT2*	This study
YSKM455	*W303a P_{CUP1-1}TAP–SRC1::KanMX6 PRP8–hub1(D22A)::natNT2*	This study
YSKM456	*W303a P_{CUP1-1}TAP–SRC1::KanMX6 PRP8–hub1–DD::natNT2*	This study
YSKM460	*W303a P_{CUP1-1}TAP–SRC1::KanMX6 SNU66–HUB1::natNT2*	This study
YSKM461	*W303a P_{CUP1-1}TAP–SRC1::KanMX6 SNU66–hub1(D22A)::natNT2*	This study
YSKM462	*W303a P_{CUP1-1}TAP–SRC1::KanMX6 SNU66–hub1–DD::natNT2*	This study
YSKM470	*W303a hub1::HIS3MX6 P_{CUP1-1}TAP–SRC1::KanMX6*	This study
YSKM471	*W303α hub1::HIS3MX6 P_{CUP1-1}TAP–SRC1::KanMX6 PRP38–HUB1::natNT2*	This study
YSKM472	*W303α hub1::HIS3MX6 P_{CUP1-1}TAP–SRC1::KanMX6 PRP38–hub1(D22A):: natNT2*	This study
YSKM473	*W303α hub1::HIS3MX6 P_{CUP1-1}TAP–SRC1::KanMX6 PRP38–hub1–DD:: natNT2*	This study
YSKM475	*W303a hub1::HIS3MX6 P_{CUP1-1}TAP–SRC1::KanMX6 PRP8–hub1(D22A):: natNT2*	This study
YSKM476	*W303α hub1::HIS3MX6 P_{CUP1-1}TAP–SRC1::KanMX6 PRP8–hub1–DD:: natNT2*	This study
YSKM477	*W303α hub1::KanMX6 Δsnu66::HIS3MX6 P_{CUP1-1}TAP–SRC1::natNT2*	This study
YSKM478	*W303a hub1::HIS3MX6 P_{CUP1-1}TAP–SRC1::KanMX6 SNU66–HUB1::natNT2*	This study
YSKM479	*W303α hub1::HIS3MX6 P_{CUP1-1}TAP–SRC1::KanMX6 SNU66–hub1(D22A):: natNT2*	This study
YSKM480	*W303a hub1::HIS3MX6 P_{CUP1-1}TAP–SRC1::KanMX6 SNU66–hub1–DD:: natNT2*	This study
YSKM498	*BY4741 prp17::KanMX6 P_{CUP1-1}TAP–SRC1::natNT2*	This study
YSKM505	*BY4741 P_{CUP1-1}TAP–SRC1::natNT2*	This study
YSKM506	*BY4741 hub1::KanMX6 P_{CUP1-1}TAP–SRC1::natNT2*	This study
YSKM513	*BY4741 bud13::KanMX6 hub1::natNT2*	This study
YSKM515	*BY4741 snu17::KanMX6 hub1::natNT2*	This study
YSKM517	*BY4741 pml1::KanMX6 hub1::natNT2*	This study
YSKM519	*BY4741 urn1::KanMX6 hub1::natNT2*	This study
YSKM524	*BY4741 ecm2::KanMX6 hub1::natNT2*	This study
	Schizosaccharomyces pombe strains	
JY741	*h^-leu1 ura4-D18 ade6-M216*	8
JY746	*h^+leu1 ura4-D18 ade6-M210*	8
YHY23P	*JY741 hub1::$aur1^R$ pUR19-$hub1^+$*	8
YHY24P	*h^-leu1 ura4-D18 ade6-M216 hub1-1-$ura4^+$*	8
YSKMSP10	*JY741xJY746 snu66::natNT2*	This study
YSKMSP12	*JY746 snu66::natNT2 pUR19-$snu66^+$*	This study

Supplementary Table 2 | Data collection and refinement statistics for Hub1-HIND crystals

	Hub1-HIND-I[a]	Hub1-HIND-II[b]
Data collection		
Space group	P1	$P2_12_12$
Cell dimensions		
a, *b*, *c* (Å)	35.23, 36.34, 83.44	36.72, 83.57, 35.11
α, β, γ (°)	83.44, 89.85, 85.84	90.0, 90.0, 90.0
Resolution (Å)	30-1.4 (1.4-1.5)*	45-1.9 (1.9-2.0)*
R_{merge}	4.5 (31.8)	6.3 (13.6)
$I/\sigma I$	25.11 (5.56)	19.04 (9.96)
Completeness (%)	94.6 (92.4)	99.4 (97.8)
Redundancy	6.86 (5.51)	6.75 (6.64)
Refinement		
Resolution (Å)	26-1.4	40-1.9
No. reflections	31992	8559
R_{work} / R_{free}	18.5 / 22.8	20.0 / 24.1
No. atoms		
Protein	1471	791
Ligand/ion	-	-
Water	294	163
B-factors		
Protein	16.25	9.52
Ligand/ion	-	-
Water	33.34	23.54
R.m.s deviations		
Bond lengths (Å)	0.007	0.008
Bond angles (°)	1.033	1.190

[a]No. of protein complexes for Hub1-HIND-I was 2.
[b]No. of protein complexes for Hub1-HIND-II was 1.
*Highest resolution shell is shown in parenthesis.

Supplementary Table 3 | Splicing-specific microarray analysis of splicing defects in *Δhub1*, *Δsnu66*, and *Δhub1 Δsnu66* yeast strains. The table is a tab-delimited file of the Intron accumulation indexes (IAI; ref. [20,21]) used for clustering in Fig. 2c.

UniqueID	*Δsnu66*	*Δhub1*	*Δhub1 Δsnu66*	*prp4-1* (37°C-1 hr)	WT
ACT1_Int	1.54256171	0.40450075	1.871173824	5.0254593	-0.1589901
ANC1-Int	-0.012090515	-0.080929737	-0.297915512	1.6189023	-0.2553241
APS3_Int	0.223265165	0.041572008	-0.258346778	2.9406543	-0.5912429
ARF2-Int	0.368301446	0.017188139	0.357370745	1.57625	-0.3727945
ARP2-Int	0.173230306	0.129185629	0.31005703	2.9126506	-0.0053954
ARP9-Int	-0.051629356	-0.06992938	-0.508016047	1.8798851	-0.2566123
ASC1_Int	0.834906167	0.096241895	0.871177978	4.108773	-0.0669337
BET1-Int	0.183035747	0.021226698	0.160052947	0.69949025	0.13034599
BIG1-Int	0.34743848	0.097609867	0.063342366	1.6873698	-0.0256485
BOS1-Int	0.436786863	-0.126122654	0.164037238	1.1068492	0.12843533
CIN2-Int	0.256009862	0.177655475	0.381001685	0.81591374	0.21243829
CNB1-Int	0.251959175	0.01876975	0.35096135	2.6016772	0.23538937
COF1-Int	0.763239074	0.481871322	0.855931301	5.059363	-0.1469866
COX4-Int	0.435361276	0.1159469	0.322435662	2.6557493	-0.2628319
COX5B-Int	0.14457474	-0.053273473	-0.167996292	1.2670034	-0.0483376
CPT1-Int	0.016575255	0.045534985	-0.173501517	0.10779375	-0.1621388
DBP2-Int	-0.033021238	-0.149231136	0.478103261	1.1733414	-0.0479762
DID4-Int	0.473848849	0.175370089	0.218139795	3.284919	-0.0590598
DMC1-Int	0.010648136	0.103370885	0.300838214	0.15678103	-0.0814317
DYN2-Int1	-0.332307295	-0.224430369	-0.155864594	2.7522867	-0.0204161
DYN2-Int2	-0.270249812	-0.216851164	-0.068356753	2.417955	-0.0883149
ECM33-Int	0.853125854	0.038876994	1.328674543	3.1235657	-0.1429699
EFB1_Int	1.166109258	0.207013074	2.829976039	2.9851568	0.04490333
EPT1-Int	0.305450134	0.243947056	0.357002506	2.5233839	-0.1787068
ERD2-Int	0.525092257	0.029352283	0.224153716	2.9231493	-0.1096932
ERV1-Int	0.20706676	-0.240493429	0.017798439	1.2110175	0.06343499
GCR1-Int	0.360346688	-0.143435948	0.707363879	0.27946123	-0.0195265
GIM5-Int	-0.088438436	-0.27964813	-0.444934221	1.8740922	0.05883049
GLC7-Int	-0.153399459	0.051604154	-0.528760951	2.395474	-0.2746456
GOT1-Int	0.819717681	-0.226976074	0.584152621	2.5723007	0.12954105
HAC1_Int	-0.251511527	0.025511191	-0.160045183	0.16957922	-0.4869207
HFM1-Int	-0.133273397	0.009176177	-0.49199712	-0.8413888	-0.0688491
HNT1-Int	0.743328187	0.036616521	0.890815845	2.685901	-0.3921309
HNT2-Int	0.265684359	0.145722266	0.741111849	0.9367185	-0.0399807
HOP2-Int	-0.14736268	0.246817387	-0.059194521	-1.8008562	0.05684986
IST1-Int	0.097186224	0.063555109	0.14594606	1.678284	-0.1172729
KIN28-Int	0.439200719	-0.094658525	0.35241477	0.8831751	0.23601161
LSM2-Int	0.142575413	0.06093282	-0.015313245	2.0938306	0.1294945
LSM7-Int	0.040937221	0.021665001	-0.594370847	3.2904975	0.00881913
MAF1-Int	0.386131877	0.463357627	-0.247544451	2.498361	-0.1204495
MEI4-Int	-0.400653342	0.243037068	0.300146196	-0.82688594	0.17098542
MMS2-Int	0.439399107	0.140655879	0.752376298	2.787141	0.1663999
MOB1-Int	0.38364375	-0.130714223	0.388685683	1.1944301	0.13033807
MOB2-Int	-0.003824938	0.055433767	-0.10611885	0.30183187	0.2227759
MPT5-Int	-0.08927689	-0.133046639	-0.199053798	1.0880322	-0.3962274
MRK1-Int	-0.000121324	0.398032738	-0.087303715	1.0705067	-0.1400227

MRPL44-Int	0.351138966	-0.222531492	0.210006619	2.4796305	-0.2818878
MTR2-Int1	-0.057310537	-0.019607398	-0.094188658	1.4717053	-0.3640847
MUD1-Int	0.191535291	0.039346573	0.54128641	1.7110869	0.10555778
NCB2-Int	0.385331202	-0.080348538	0.037962237	1.5961785	0.27464938
NCE101-Int	0.323516851	0.110773375	0.303662108	1.139717	0.04765657
NHP6B-Int	0.597910981	0.054813968	0.091193731	1.8091354	-0.0601715
NMD2-Int	-0.209829069	0.095133648	-0.318451519	2.6144547	-0.0370925
NSP1-Int	0.283556658	0.04858973	0.366541627	1.8901703	-0.1538525
NYV1-Int	0.61119942	0.073973059	0.168009436	3.0221395	-0.0920492
OST5-Int	0.451924972	0.073901321	0.320557824	1.7518047	0.11105923
PCH2-Int	-0.255970852	-0.157196687	-0.585974704	-0.675492	0.20896488
PFY1-Int	0.776706998	-0.120817856	0.604038054	1.5815822	0.05545277
PHO85-Int	0.216577879	0.103946309	0.558168366	1.5132025	-0.0353904
PMI40-Int	0.567114263	0.012351919	0.701977272	2.0533264	-0.0319671
POP8-Int	0.312725622	-0.174779836	0.282743302	2.7176554	-0.0473417
PRE3-Int	1.015498522	0.069392095	0.861987242	2.7353895	0.29532692
QCR10-Int	0.642283781	0.591548912	1.388436248	2.4626453	-0.0826485
QCR9-Int	0.597225015	0.13726197	0.379102819	3.2581627	0.00217896
RAD14-Int	0.037036041	-0.246585982	0.143982496	0.93910897	-0.1665642
REC107-Int	0.032730272	-0.047648125	0.065011666	0.00188337	0.06749329
REC114-Int	-0.15164415	0.003760482	-1.473646225	3.1246703	-0.0217286
RFA2-Int	0.10468027	0.052370785	0.348469243	1.0379936	0.09285116
RIM1-Int	0.750173769	0.118339283	0.501612755	3.670782	0.03300926
RPL13A-Int	0.396311742	-0.067913329	0.877008838	3.4049463	-0.5072034
RPL13B-Int	0.212355855	-0.060487623	0.849753791	3.3050237	-0.3808198
RPL14A-Int	1.064334916	-0.219635234	1.1319329	3.8665059	0.4254974
RPL14B-Int	0.460538727	-0.135344273	0.421788583	3.2299654	0.29592967
RPL16A-Int	0.285666946	-0.022152125	0.561982836	3.0379286	-0.3293016
RPL16B-Int	0.276388908	-0.228092728	-0.189374191	4.1564636	-0.2995686
RPL17A-Int	0.327960734	0.092083378	0.40617667	4.011033	0.07008811
RPL17B-Int	0.95608016	-0.029461991	1.195295248	3.3237073	0.186372
RPL18A-Int	0.239763025	-0.13863452	0.610811452	3.50373	-0.1323904
RPL18B-Int	0.258911325	-0.081987639	0.49489072	1.2664522	0.21757583
RPL19A-Int	0.225314548	0.134703438	0.549508261	3.8266692	-0.4526924
RPL19B-Int	0.062441406	-0.022552583	0.091711376	3.3872354	-0.3415878
RPL20B-Int	0.146477421	-0.249853369	-0.001591167	3.5278845	-0.3555637
RPL21A-Int	0.348202909	0.210984142	0.604024304	4.1027737	-0.2383207
RPL21B-Int	0.484053882	-0.000916262	0.918297219	4.5532417	-0.1579632
RPL22A-Int	0.494084021	-0.212273243	1.277779832	3.250872	0.03200427
RPL22B-Int	-0.143650879	-0.064885006	0.468918846	0.34410492	0.16128159
RPL23A-Int	0.321202396	0.174885669	0.097761018	3.1183515	-0.0213206
RPL23B-Int	0.207597918	-0.194072376	0.388353206	3.272361	-0.0062148
RPL24A-Int	0.147442224	-0.010086169	0.139446006	2.5341823	-0.2263903
RPL24B-Int	0.201788775	0.056177971	0.133719599	3.1854913	-0.4755634
RPL25-Int	0.377885018	-0.185748837	0.383432121	4.5896873	-0.4820382
RPL26A-Int	0.441481784	-0.014922194	0.517693942	3.8166537	0.17650619
RPL26B-Int	0.439994447	0.041031535	0.747473286	3.7175355	-0.1339706
RPL27A-Int	0.178538863	0.021071432	-0.28920189	4.2789335	-0.0979038
RPL27B-Int	0.424366429	-0.032738169	0.012886149	2.9366796	0.22010101

RPL28-Int	0.622334396	0.127684585	1.512921146	2.3489535	0.23165286
RPL29-Int	0.056212867	-0.166672122	-0.361748585	3.5906372	-0.0073817
RPL2A-Int	1.108536408	0.052015171	1.648358602	2.400238	0.21001083
RPL2B-Int	0.91299546	0.041672633	1.216019132	3.5596771	-0.1100236
RPL30-Int	1.310401402	0.512510043	2.17048151	3.3412087	0.12324465
RPL31A-Int	0.088231345	-0.222070993	0.121892865	4.3277245	-3.35E-04
RPL31B-Int	0.11854743	-0.058531571	-0.344321707	2.9449034	0.11823431
RPL32-Int	0.292206054	-0.004681615	0.347658561	3.7369342	-0.0672212
RPL33A-Int	0.765534302	0.002198135	0.997859891	4.3796167	-0.1153155
RPL33B-Int	0.242280049	-0.073069165	0.470751422	4.5108013	-0.2453709
RPL34A-Int	0.373754721	0.165980839	0.907756582	3.2413516	0.12980059
RPL34B-Int	1.059228287	1.625409535	2.404761595	3.2217288	0.2601812
RPL35A-Int	0.194635072	-0.089714993	0.249163621	3.9169016	-0.1650231
RPL35B-Int	0.270398832	-0.034998037	0.297601923	3.883262	-0.2693453
RPL36A-Int	0.104860671	-0.07175125	0.176184249	2.5679374	0.04617317
RPL36B-Int	0.496233407	0.133066701	0.750411221	4.200331	-0.0574329
RPL37A-Int	0.421026421	-0.056483632	0.916877469	4.69133	0.21791305
RPL37B-Int	0.495485495	-0.016241563	0.603662342	3.9818969	0.13027442
RPL39-Int	0.211669521	-0.124795473	0.288496366	5.583402	-0.0180505
RPL40A-Int	0.359493877	-0.519626448	0.564439357	2.5436385	-0.0819435
RPL40B-Int	0.23873967	-0.046223339	0.492011119	3.0734766	-0.2337821
RPL42A-Int	0.032498901	0.138562749	0.304428851	3.5811882	-0.0060746
RPL42B-Int	0.107565976	-0.269269135	-0.087519389	2.7080107	0.3316299
RPL43A-Int	0.520742853	-0.164011037	0.61679524	3.7519135	0.00469579
RPL43B-Int	1.191856427	-0.093935393	1.491349739	4.9954295	0.10420418
RPL6A-Int	0.134674904	-0.283363139	0.591709196	3.753131	0.2017046
RPL6B-Int	0.156659492	-0.124921236	0.339093807	3.4438198	0.03586953
RPL7A_Int2	0.594945498	-0.060197878	1.149362739	3.6972349	-0.2948796
RPL7A-Int1	1.158654723	-0.163388416	2.02064625	3.4880831	-0.1631177
RPL7B_Int2	0.476669997	0.164801541	1.419782619	3.0983238	-0.3171785
RPL7B-Int1	0.245393144	0.158565812	0.977651349	2.0072303	-0.2161085
RPO26_Int	0.342754897	-0.132803136	-0.120151847	2.904333	-0.1288532
RPP1B_Int	0.472896447	-0.364451144	0.108522803	4.017258	0.02127471
RPS0A-Int	0.346858898	-0.040857496	0.948323716	3.4126766	-0.085314
RPS0B-Int	0.117937996	0.158404405	0.320093105	4.1349807	-0.2911967
RPS10A-Int	0.251276666	-0.140307382	0.050518847	4.809004	0.02403696
RPS10B-Int	0.309156023	0.16636125	0.197494687	3.588964	0.0410374
RPS11A-Int	0.725752024	-0.020770612	1.475612565	3.8669019	-0.0701192
RPS11B-Int	0.726313529	0.030390456	0.872639511	2.7181969	0.30428734
RPS13-Int	0.593258181	0.019134554	0.856950529	2.625484	0.24176092
RPS14A-Int	0.548834238	0.305362191	0.549256668	3.731258	-0.159917
RPS14B-Int	0.498047273	-0.06134746	1.636791528	2.3870625	0.28607655
RPS16A-Int	0.569838906	-0.089234805	0.819195775	4.2838073	0.11090397
RPS16B-Int	0.387283793	-0.023860932	0.174118751	3.4873643	-0.1459322
RPS17A-Int	0.052772179	-0.141985632	0.286384836	3.9673193	-0.0605855
RPS17B-Int	0.178136488	-0.094546513	-0.324724939	3.6530461	-0.2129112
RPS18A-Int	-0.009148648	0.106613683	0.352732635	4.378755	-0.35989
RPS18B-Int	0.20036574	0.031832388	0.466497192	3.8886852	-0.4813297
RPS19A-Int	0.015827065	-0.083056311	0.087284067	4.6144443	0.09739469

RPS19B-Int	0.484934605	-0.00459326	0.434769502	4.4119725	-0.111377
RPS21A-Int	0.533908383	-0.054374197	0.40223713	4.040518	0.02745374
RPS21B-Int	0.764485005	-0.26170915	0.659690143	4.0666146	0.08249677
RPS22B-Int1	0.728803992	-0.332386615	1.266399896	1.4549052	-0.0658066
RPS23A-Int	0.276298364	0.043936252	-0.03601854	3.4035869	0.06793448
RPS23B-Int	0.32214751	-0.271392402	0.194710291	3.5310347	-0.2273517
RPS24A-Int	0.569669159	0.010964672	0.707460918	4.365769	-0.2574035
RPS24B-Int	0.182894549	0.124561192	0.157473821	2.5287573	-0.2535567
RPS25A-Int	0.920201773	-0.003466909	1.154311635	3.7408073	-0.0855614
RPS25B-Int	0.279703671	-0.055610584	0.354553175	3.4662097	-0.0126323
RPS26A-Int	0.926884052	-0.069474587	0.976864969	5.0427184	-0.2124602
RPS26B-Int	0.448930383	0.285431959	0.589748563	3.3583186	0.0373675
RPS27A-Int	0.283870492	0.006970731	-0.216873431	2.5468988	-0.1691602
RPS27B-Int	0.593378146	0.120721938	0.189295981	4.64516	0.11253479
RPS29A_Int	0.39875246	-0.131348141	0.540806634	4.4607573	-0.071763
RPS29B_Int	0.433465136	-0.151212837	0.56963054	3.4870336	-0.0047564
RPS30A-Int	0.147999898	0.110317428	-0.097686824	3.4470577	-0.0256989
RPS30B-Int	0.916975219	0.206929166	1.178198003	3.827842	0.21077819
RPS4A-Int	0.914071882	-0.521201649	1.17446191	4.255475	-0.06334
RPS4B-Int	0.377126588	0.235166093	0.935216622	3.9450524	-0.115894
RPS6A-Int	0.341152329	-0.17384298	0.887086128	3.909064	-0.4457887
RPS6B-Int	0.249254458	-0.068801145	0.169635609	3.3097866	-0.5691597
RPS7A-Int	0.322513303	-0.046116104	0.269003535	4.26799	-0.0841948
RPS7B-Int	0.104669342	0.183510905	0.348190217	3.309974	-0.1120999
RPS8A-Int	0.242267952	0.21180158	0.915578676	3.4946377	-0.5560538
RPS8B-Int	0.657169643	0.222581138	0.970556465	3.3290122	-0.2189676
RPS9A-Int	0.122258104	0.092644283	0.412332182	0.559549	-0.0603522
RPS9B-Int	0.691960927	-0.066238449	0.992147342	3.113941	-0.0725942
RUB1-Int	0.092211351	-0.286044078	-0.111648455	2.879541	2.58E-04
SAC6-Int	0.297386997	-0.404192297	0.378548193	1.2502017	-0.0402485
SAR1-Int	0.607345343	-0.001272203	0.120634599	4.3237376	-0.0152237
SEC14-Int	0.751220569	0.149407621	1.330958974	2.4984608	1.2877363
SEC17-Int	0.431434769	0.28522688	0.502727009	2.2591393	-0.0946854
SEC27-Int	0.809963785	0.096881326	0.947069942	2.325161	-0.1593422
SFT1-Int	0.27285797	0.247090206	-0.041746373	1.119859	0.17272691
SMD2-Int	0.080474229	0.001400658	-0.200087462	1.3153604	-0.1244774
SNC1-Int	0.389189607	0.078773539	0.27427071	3.127336	0.09135673
SNR17A-Int	0.958498578	0.116232202	0.141547382	2.8815942	-0.1830912
SNR17B-Int	1.820652092	0.027131072	0.878341242	2.1577873	-0.3645747
SPO1-Int	-0.304132477	0.02573556	-0.163467665	0.15857534	0.0062248
SPO70_Int	0.028083026	0.13320085	-0.024092659	-0.23340176	-0.0880876
SPT14-Int	-0.048752726	-0.060572494	0.220692561	1.1048923	-0.1281037
SRB2-Int	0.795514052	0.371055162	1.014857779	0.06826691	0.25869083
SRC1-Int	0.464221044	-0.430561125	0.478390604	1.4238423	0.12041573
STO1-Int	0.039558542	0.064277565	0.063757218	1.71706	0.08980615
TAD3-Int1	0.053220489	0.006938803	-0.088653388	2.17152	0.17471895
TAD3-Int2	-0.052122587	0.126539382	0.142437593	1.7322667	0.16057634
TEF4_Int	1.367919691	0.146841195	1.805580128	3.2483253	-0.0355725
TFC3-Int	0.588576618	0.297171338	0.51613018	0.6791669	-0.2127539

TUB1-Int	0.689975691	-0.053486198	1.255744011	4.291914	-0.3759881
TUB3_Int	0.48496912	-0.217362052	0.434296124	2.186179	0.04503803
UBC12-Int	0.176035534	0.206801387	-0.010950942	1.0530851	0.04505568
UBC13-Int	0.305217609	0.157103195	0.433516856	1.8727603	0.13954774
UBC4-Int	0.687244188	-0.099821329	0.999464725	3.5976732	-0.3222416
UBC5-Int	0.385959124	0.136671179	-0.701499544	-1.8385911	0.04642136
UBC8-Int	-0.132286892	-0.127525393	-0.263058523	1.3352295	-0.1585498
UBC9-Int	0.376544299	0.003870127	0.696974533	1.5428294	0.00655999
VMA10-Int	0.453329092	-0.094509387	0.070885207	3.8203282	-0.1433687
VPS29-Int	0.195531114	0.229390268	0.251936996	2.023372	0.00572053
YBL059C-A_Int	0.540257526	0.109537884	1.133758309	2.8660836	-0.1103957
YBL059W-Int	0.064870741	-0.210826629	-0.081909153	1.3089828	0.38141805
YBL091C-A_Int	0.039130227	0.211785801	-0.323994533		0.1097345
YBR230C-Int	1.142346747	0.204421781	0.540818512	2.923409	-0.0858824
YBR255C-A_Int	0.763235862	0.05936503	1.144366671		0.09544664
YDL012C-Int	0.895618792	-0.030643651	1.057631208	2.2378898	0.17457937
YDL115C-Int	0.105569539	0.181879852	0.104196441	0.85771126	-0.1333722
YDL189W-Int	0.231238271	0.149372076	0.547664279	0.46563396	-0.2137218
YDL219W_Int	0.12015067	0.088700263	0.368433535	3.4869115	-0.0922589
YDR367W-Int	0.298742937	-0.142661225	0.237863995	2.1553051	0.48053434
YDR381C-A_Int	-0.146703491	-0.000180446	0.107571892		-0.0284919
YER007C-A-Int	0.386923213	0.11364718	0.150768889	2.2425475	-0.2783083
YER074W-A_Int1	0.197266578	0.001232173	-0.407586904		-0.0482203
YER074W-A_Int2	0.496909739	0.119254627	0.351112159		-0.3942766
YER093C-A-Int	0.233760358	0.098269002	0.103161143	1.4898459	0.22274278
YFR024C-A-Int	0.704011994	-0.057506865	1.040854399	2.4777546	-0.1233998
YGL232W-Int	0.160651874	-0.198441371	0.285527318	0.7176348	-0.1645745
YGR001C-Int1	0.156861022	0.039149169	0.017829348	1.4288207	0.0757716
YGR001C-Int2	0.193489415	-0.174886314	0.008331546	3.4062896	0.11208105
YHR079C-A_Int	-0.282484461	0.195753291	-0.102445706		0.06449805
YHR097C_Int	0.264591594	-0.024249294	0.502182247	1.661401	0.04948932
YIP2-Int	0.643584179	0.084001791	0.596863553	3.0849202	0.18342073
YIP3-Int	1.063237182	0.418113488	1.518818395	2.9579163	-0.0049314
YKL158W-Int	0.101039126	0.135617761	0.269742778	1.1517327	-0.0607781
YKR095W-A_Int	0.366462991	0.069982255	0.826182989		0.06409005
YLR128W-Int	0.084753221	0.072568511	0.398005311	1.8434483	-0.0957653
YLR211C-Int	-0.070733229	0.14404035	0.037431379	0.08417026	-0.1186131
YLR426W-Int	0.150123882	-0.136093259	-0.049542363	0.8330456	-0.1587888
YML025C-Int	0.601541318	0.262348711	0.324322648	1.6701928	0.12390108
YML067C-Int	0.334123519	0.141887045	0.112408066	2.846613	-0.0881944
YNL050C-Int	-0.134338884	-0.074673162	-0.065216087	1.0460563	0.01109719
YNL246W-Int	0.529222676	-0.13438444	0.472126096	2.3762631	-0.1396986
YNR053C_Int	0.302742558	0.194477592	1.780062818	-0.38714257	-0.2845221
YOL047C-Int	0.063445718	0.299575289	-0.107056531	-0.15497248	0.32162502
YOL048C_Int	0.202465236	0.185802976	0.688762397		
YPR063C-Int	0.850237252	0.156812061	0.684527526	2.1201954	0.03229143
YPR098C_Int	0.447134885	0.170719485	0.302178248		0.09070747
YRA1-Int	-0.178319039	-0.081449487	0.223839901	1.4883447	0.03947612
YSC84-Int	0.280640483	0.024728911	-0.054296015	1.1193012	0.08100308

Supplementary References

45. Costanzo, M. *et al.* The genetic landscape of a cell. *Science* **327,** 425-431 (2010).
46. Decourty, L. *et al.* Linking functionally related genes by sensitive and quantitative characterization of genetic interaction profiles. *Proc. Natl. Acad. Sci. USA* **105,** 5821-5826 (2008).
47. Umen, J. G. & Guthrie, C. Mutagenesis of the yeast gene PRP8 reveals domains governing the specificity and fidelity of 3' splice site selection. *Genetics* **143,** 723-739 (1996).
48. Dahlmann, M. Die Funktion des Ubiquitin-ähnlichen Proteins Hub1 in S. cerevisiae. *PhD Thesis* Freie Universität Berlin (2008).
49. Macias, S., Bragulat, M., Tardiff, D. F. & Vilardell, J. L30 binds the nascent RPL30 transcript to repress U2 snRNP recruitment. *Mol. Cell* **30,** 732-742 (2008).
50. Tong, A. H. *et al.* Systematic genetic analysis with ordered arrays of yeast deletion mutants. *Science* **294**, 2364-2368 (2001).
51. Ulrich, H. D. & Jentsch, S. Two RING finger proteins mediate cooperation between ubiquitin-conjugating enzymes in DNA repair. *EMBO J.* **19,** 3388-3397 (2000).
52. James, P., Halladay, J. & Craig, E. A. Genomic libraries and a host strain designed for highly efficient two-hybrid selection in yeast. *Genetics* **144,** 1425-1436 (1996).